

Rejection of Input Distributions in the Buck Converter through the Feedforward Digital Controller

Lucas M. de Lacerda ^{a*}, Fabiano L. Cardoso ^a,

^a Universidade do Estado de Santa Catarina (UDESC),
Paulo Malschitzki street, 200 - North Industrial Zone,
Joinville – SC, Brazil, Zip Code 89219-710.

Mellyssa S. de Souza ^b

^b Universidade Federal do Rio de Janeiro (UFRJ),
Cidade Universitária, Rio de Janeiro - RJ,
Brazil, Zip Code 21941-972.

Abstract: This article presents the advantages of using the feedforward controller in switched DC-DC converters to increase the rejection ratio to the input voltage-related disturbances of the converter. The controller analysis and design procedure are also presented. Through simulations, the feedforward controller is compared with other techniques based only on feedback control of the output voltage.

Key words: DC-DC Buck converter, voltage lowering converter, digital control, feedforward control.

INTRODUCTION

Today, electronic power converters play an important key role in how electricity is processed in many applications. DC-DC static converters are devices that receive a voltage or direct current level at their input terminals and adjust to another voltage or direct current value at the output terminals according to system requirements. There are three basic topologies of DC-DC static converters: Buck (voltage down), Boost (voltage lifter) and Buck-Boost (voltage down-lifter) [1]. These converters are widely used in computers, hybrid power systems, uninterrupted power supplies, regulated sources, electric vehicles, among other systems [2]. For the control of the flow of energy between a source of continuous voltage and the load with characteristics of voltage source, an inductive accumulation type converter is used. In this case, among the several topologies that operate with this premise is the Buck converter [3]. Buck converters are used in many applications, generally aiming to keep the input voltage at constant output levels even in the face of load fluctuations [4,5]. They are still used in applications where there is a single power supply and a need for different voltage levels for various circuits [1]. Buck converters are applied in systems that operate with solar and / or wind power generation, aiming to maintain constant output voltage even with oscillations in the input voltage. Compared to linear voltage regulators, DC-DC converters feature better performance and greater compaction capacity and are preferred in most modern applications for signal conditioning above a few tens of watts of power. Considering the above, in this work one of the digital control techniques for the downconverter is studied so that the output voltage remains constant regardless of input voltage variations (input disturbance rejection).

1. MODELING OF THE PLANT

The modeling of the Buck converter, shown in Figure 1, has been widely discussed in the literature [6]. In general, these

models differ from each other in mode of operation of the converter (continuous or discontinuous), form of equation of the model (differential equations, state space or s-plane), retraction of the non-idealities of the circuit, and the variable to be controlled (cyclic ratio, load or input voltage) [3-10]. The topology of the DC-DC Buck converter is shown in Figure 1, where: V_i is the input voltage, S is the static switch, D is a diode, L is an inductor for energy storage, C is a capacitor that acts as an output filter, $i_L(t)$ is the current on the inductor, and V_o is the output voltage supplied to the load R.

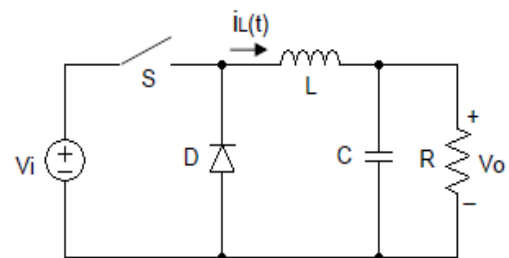


Figure 1 - Topology of the DC-DC Buck converter.

In this work the modeling presented by Erickson [5] and Barbi [6] will be used. In the modeling, the relation between the output voltage of the converter (V_o) and the cyclic ratio (d) is made by analyzing the behavior of voltages and currents in the circuit for the steps of operation of the converter. The technique of analysis of instantaneous average values is also applied within a converter switching cycle. Equations 1 and 2, which represent the dynamic behavior of the Buck converter, are obtained through nodal and mesh analysis of the equivalent electric circuit.

$$L \frac{di_L(t)}{dt} = -V_o(t) + d(t)V_i(t) \quad (1)$$

$$C \frac{dV_o(t)}{dt} = i_L(t) - \frac{V_o(t)}{R} \quad (2)$$

Equation 3 relates the input and output voltage as well as the transfer function of the converter through the ratio of the output voltage of the converter to the cyclic ratio as presented in Equation 4.

$$\frac{v_o(s)}{v_i(s)} = d \quad (3)$$

$$\frac{v(s)}{d(s)} = \frac{V_i}{LCs^2 + \frac{L}{R}s + 1} = \frac{V_i/LC}{s^2 + \frac{1}{RC}s + \frac{1}{LC}} \quad (4)$$

In Equation 4, $d(s)$ is the cyclic operating ratio of the converter related to the time that the S-key (Figure 1) is in conduction with the total switching period of the DC-DC converter. According to Bezerra [2], the generic state space representation is given by Equation 5.

$$\begin{aligned} \dot{x}(t) &= Ax(t) + Bu(t) \\ y(t) &= Cx(t) + Du(t) \end{aligned} \quad (5)$$

From the differential equations of the system, it is possible to perform state space representation and transfer function. The state variables X_1 and X_2 are defined as the current in the inductor (i_L) and the voltage in the capacitor (V_C) respectively. As input to the system is the input voltage (V_i) and output voltage at the capacitor (V_C).

For the modeling and representation of the system in space of state, the average model of the Buck converter is used, neglecting the switching harmonics and the nonlinearities present in the model [7,8,9]. The space of state representation is given by Equations 6 and 7.

$$\begin{bmatrix} \dot{i}_L \\ \dot{V}_C \end{bmatrix} = \begin{bmatrix} 0 & -\frac{1}{L} \\ \frac{1}{C} & -\frac{1}{RC} \end{bmatrix} \begin{bmatrix} i_L \\ V_C \end{bmatrix} + \begin{bmatrix} d \\ 0 \end{bmatrix} V_i \quad (6)$$

$$V_o = [0 \quad 1] \begin{bmatrix} i_L \\ V_C \end{bmatrix} \quad (7)$$

Where:

- i_L : inductor current
- V_C : capacitor voltage
- V_i : input voltage
- V_o : output voltage (V_C)

As can be observed in Equations 6 and 7, by adjusting the cycle of work, the voltage at the output can be controlled.

2. Buck converter operating with digital control

According to Ogata [12], the control of any system is based on the analysis of the block diagram that represents it. The block diagram is a graphical representation that allows to identify and individualize the elements that make up the system. Figure 2 shows the block diagram for the proposed Buck digital control converter.

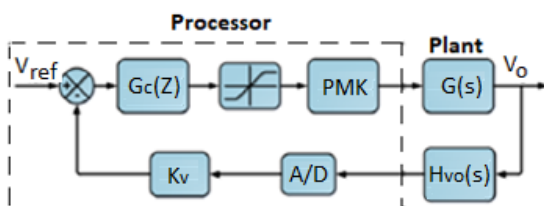


Figure 2 - Block diagram of the Buck converter with digital control [8].

$G(s)$ is the transfer function representing the Buck converter, also called the plant. $H_{vo}(s)$ is the transfer function of the

voltage feedback loop. The voltage feedback loop may contain, in addition to the gain of the sensor, a filter for eliminating the ripple of the output voltage. Besides the blocks shown in Figure 2, there are others inside the processor that will perform the digital control of the converter. V_{ref} is the reference voltage for the output voltage. A/D is the digital analog converter that converts the output of the output voltage sensor to a digital value. The A/D transfer function is a gain (K_{AD}) that depends on the bit resolution of the processor's converter. K_v is a gain given the value coming from the A/D to keep it in the same order of magnitude of V_{ref} . In this work, the gain resulting from the multiplication of the gains of the digital analog converter and K_v will be considered equal to 1. $G_c(z)$ is a digital controller implemented in the processor through the differential equations. The saturator has the main function of limiting the input value of the PWM modulator and avoiding high control efforts with the consequent wind-up problem [4,5]. The PWM modulator has the function of generating the switching signal for switch S (Figure 1) from the output signal of the controller. Due to the system being discrete, the output of the PWM is updated from the last value available for the output of the controller/saturator. This behavior produces a delay in the propagation of the signal, or rather, the cyclic ratio at a given moment is defined with the values of the last calculation performed by the processor. In this way, the PWM is modulated as an ideal signal retarder. Considering the sampling frequency of the A/D converter the same as the switching frequency of the converter, it can be concluded that the PWM delay is one switching cycle.

Although it is digital, this form of control follows the classic control methodology of the Buck converter in the continuous domain. Due to this, input voltage fluctuations pass through the set converter and control going to the output, varying the V_o signal. With the variation of V_o , the control detects errors in the output signal in relation to the reference signal. Thus, the control acts by correcting the output voltage to change the cyclic ratio d . This action of the system is called feedback [4]. The filter in the feedback loop to eliminate ripples and noise makes the control action slower in these cases.

According to the classical design methodology, the controller for a Buck converter is generally designed through the frequency response of the converter and the controller is in general PI (Proportional Integral) [5,7]. To improve the dynamic response of the system in relation to the noise rejection or oscillation capacity in the input voltage, it is proposed that a forward controller be implemented in the converter control structure. According to Redl [14], the feedforward control is a simple form of control that presents high efficiency and improves the degree of robustness of the system. This is a poorly exploited technique in switched-mode converters with a focus on regulation although it is a very interesting feature for large disturbances in the input signal.

The feedforward control measures the disturbance variables and takes the corrective actions before they affect the process. However, the forward control has the following disadvantages: the necessity of online measurement of the variables is subject to the disturbances, implying higher costs; and 2) the quality of

the control is directly related to the precision of the model used and, finally, depends on the knowledge of the process dynamics in response to the disturbances [13,15]. According to Lucas [16], the use of the feedforward controller has the advantage of reducing the steady state error if the Buck converter is being controlled in state space without the inclusion of an integral term in the control.

Considering the above, aiming at a better response of the Buck converter to disturbances in the converter supply voltage, a feedforward control structure shown in Figure 3 is proposed, where the input voltage is sampled and taken to the forward $G_F(z)$ controller, which will act directly in the cyclic ratio of the converter even before the output has been affected by the oscillation in the input voltage (V_i).

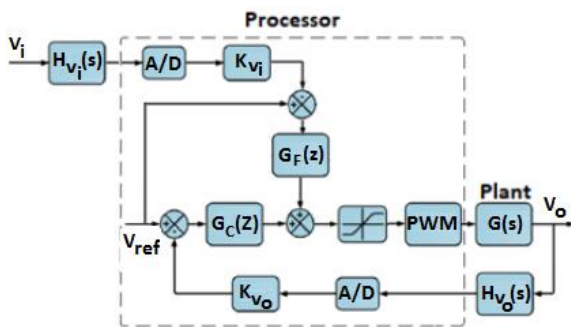


Figure 3 - Diagram of Buck converter blocks with mesh feedforward control.

In this type of control, the gains given in the sampled signal V_i cause the difference between the sampled signal and the reference signal to be zero. Thus, $G_F(z)$ has zero output and does not interfere in the performance of the $G_C(z)$ controller, which is the closed loop controller. However, if the input voltage drops, the error signal is positive and $G_F(z)$ will have a positive output, increasing the cyclic ratio of the DC-DC converter. Thus, the ratio of the output signal to the input increases. An analogous actuation occurs when the input voltage takes values greater than the nominal values.

3. PLANT DEFINITION

The Buck converter used to test the feedforward control has the specification of its parameters based on typical values that can be found in applications where banks of batteries are used, photovoltaic panels susceptible to variation of light intensity, whether due to time of day, season of the year, or even by clouds; or even in applications with small wind generators susceptible to variations in wind pressure. In these applications the input voltage may vary depending on whether the operating cycle is charge or discharge. In this way, the variables and their respective values for the converter design used in this article are represented in Table 1.

Table 1 - Data of the Buck converter.

Variable	Description	Value	Unit
V_i	Input voltage	$96 \pm 20\%$	V
V_o	Output voltage	48	V
f_s	PWM switching frequency	50	kHz
d	Cyclic ratio	0,5	-
P	Power	1000	W
R	Electrical resistance	2,304	Ω
L	Inductance	48	mH
C	Capacitance	1,25	μF
Δi	Ripple of current in the inductor	1	A
Δv	Ripple voltage on the capacitor	2	V

Details for the design of the Buck converter components are presented by Barbi [6]. In Equations 8 and 9 the resulting state space representation is given.

$$\begin{bmatrix} \dot{i}_L \\ \dot{V}_C \end{bmatrix} = \begin{bmatrix} 0 & -2083,3 \\ 0,8 \cdot 10^6 & -3,4722 \cdot 10^5 \end{bmatrix} \begin{bmatrix} i_L \\ V_C \end{bmatrix} + \begin{bmatrix} 1157 \\ 0 \end{bmatrix} V_i \quad (8)$$

$$y = \begin{bmatrix} 0 & 1 \end{bmatrix} \begin{bmatrix} i_L \\ V_C \end{bmatrix} + 0 V_i \quad (9)$$

In Equation 10 the transfer function in the frequency domain is given.

$$\frac{V_o(s)}{d(s)} = \frac{96}{6 \cdot 10^{-10}s + 2,0833 \cdot 10^{-4}s + 1} \quad (10)$$

4.1 - Open-Loop continuous system response

In order to obtain the response of the open-loop system with a unitary step, the response of the same was simulated in MATLAB software, as presented in Figure 4.

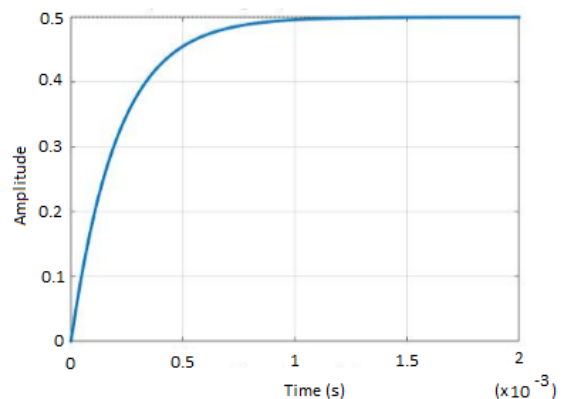


Figure 4 - Unit step response to the open-loop continuous system.

As shown in Figure 4, the system presents stable behavior in open loop for input voltage and constant cyclic ratio in steady state.

Figure 5 was obtained through the PSIM electronic version simulator, version 9.1, which shows the system operating in an open loop with an input disturbance of approximately 10% added to the signal “ V_i ” in the form of steps.

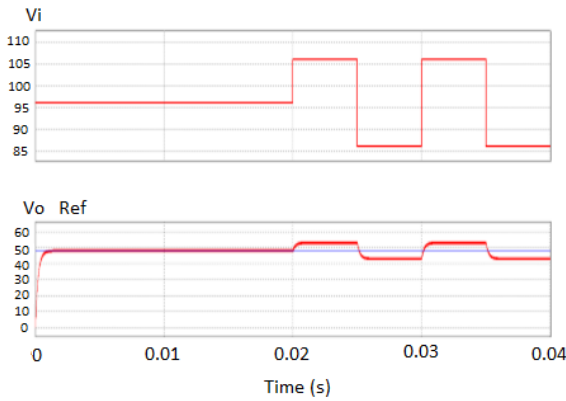


Figure 5 - Behavior of the open-loop system in relation to disturbances in the input voltage in the form of steps.

Figure 6 shows the open-loop system with a continuous input disturbance added to the “Vi” signal of approximately 10% in the sinusoidal form. The open-loop system does not have the ability to reject input disturbances properly, resulting in oscillation of the system output voltage. Thus, it is necessary to design a control system capable of stabilizing the output voltage from the control of the cyclic ratio of operation of the converter in order to make the output voltage immune to fluctuations of the input voltage.

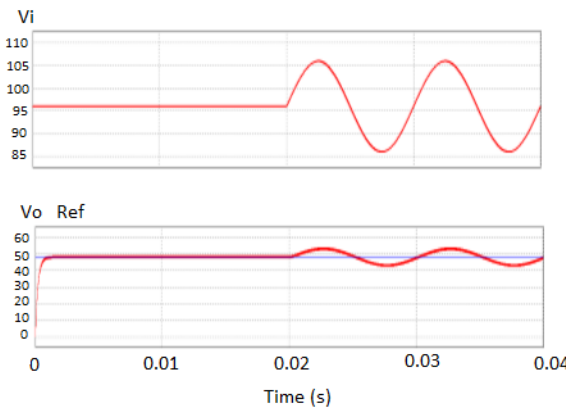


Figure 6 - Behavior of the open-loop system in relation to perturbations in the input voltage in sinusoidal form.

The discretization of the transfer function of the continuous system of the Buck converter represented in Equation 10 is performed by MATLAB using the zero-order hold (ZOH) and sampling time of 50 ms. The discrete-time transfer function of the converter is represented by Equation 11.

$$G_{conv}(z) = \frac{7,652 z + 1,245}{z^2 - 0,983 z + 0,964 \cdot 10^{-3}} \quad (11)$$

The discretized matrices A, B, C, and D are represented respectively in Equations 12, 13, 14, and 15.

$$A_d = \begin{bmatrix} 0,9203 & -5,594 \cdot 10^{-3} \\ 2,148 & -0,01201 \end{bmatrix} \quad (12)$$

$$B_d = \begin{bmatrix} 0,02233 \\ 0,04428 \end{bmatrix} \quad (13)$$

$$C_d = [0 \quad 1] \quad (14)$$

$$D_d = [0] \quad (15)$$

Figure 7 shows the comparison between the continuous and discrete system responses for the input unit step type.

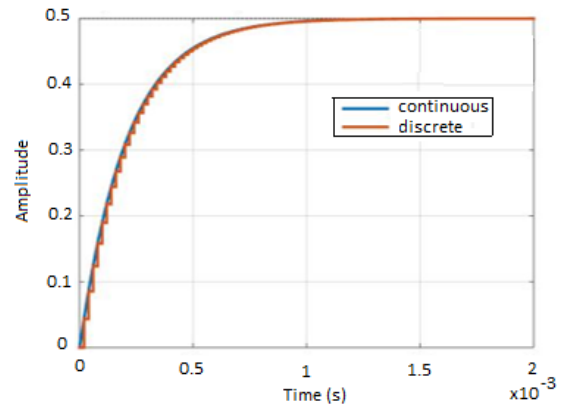


Figure 7 - Unit step response to the continuous and discretized systems.

According to Ogata [12], the stability of a discrete system can be evaluated from the location of its poles, which are the roots of the denominator of the transfer function. The discrete system response will be stable when $|\lambda| < 1$.

From the graphical representation of the geometric place of the roots in Figure 8, it is observed that the system is stable; however, with the increase in closed loop gain, a pole tends to leave the unit circle, leading the system to instability.

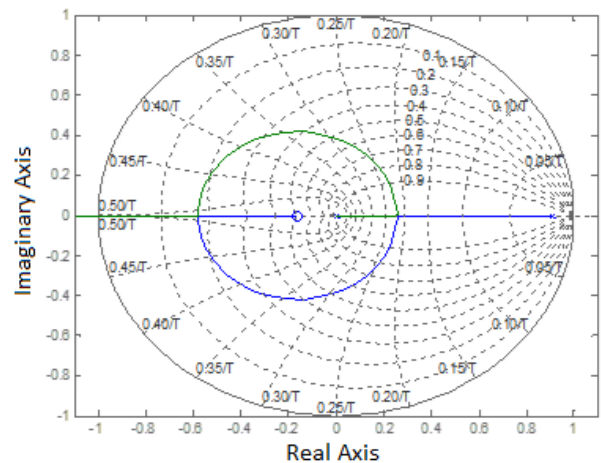


Figure 8 - Geometric Place of Roots for the discrete system in open mesh.

The poles of the discrete system are presented in Equation 16 and zeros in Equation 17.

$$\begin{aligned} \lambda_1 &= 1,06 \cdot 10^{-3} \\ \lambda_2 &= 0,9072 \end{aligned} \quad (16)$$

$$zero = -0,163 \quad (17)$$

With respect to the controllability and observability of the system, there are several ways of performing such analyses. The most common form is the rank analysis of controllability and observability matrices. Using the “ctrb” and “obsv” commands of MATLAB, it is possible to generate the matrices of controllability and observability, respectively. Through the analysis of the station of such matrices, it is concluded that the system is fully controllable and observable.

The switching ratio of “S” in the Buck converter depends on the cyclic ratio “d” imposed by the pulse width modulator (PWM). The discretization of the PWM modulator generally is described as a pure delay of one unit of the switching cycle. The transfer function of the PWM modulator is represented in Equation 18.

$$G_{pwm}(z) = \frac{1}{z} \quad (18)$$

The delay value can be changed according to the ratio of the sampling frequency of the system and the switching frequency of the converter. The discretization of the control blocks that are modeled as just a gain, remain only a gain of the same value even after the discretization. The discrete controller designed through the MATLAB auto-tuning tool is a PI (Proportional Integral) whose transfer function is presented in Equation 19.

$$G_c(z) = 2,9745 + \frac{0,4417}{z-1} \quad (19)$$

4. FEEDFORWARD CONTROLLER DESIGN

The design of the feedforward controller for the Buck converter presented in this article aims to ensure a good ability to reject input voltage variations. In this case the controller aims to keep the output voltage of the converter constant even with variation in the input voltage, allowing its use in the applications described in item 1. The sensor gains at the input voltage, $H_{Vi}(s)$, will cause the maximum voltage at the input of the processor to be compatible with the maximum allowable voltage across the A/D converter. The gain of the A/D converter (KAD) is given by the conversion ratio of the A/D converter as a function of its number of bits. The gain k_{vi} is determined such that the operating voltage is in accordance with Equation 20.

$$V_{ref} = H_{Vi}(s) \cdot K_{AD} \cdot K_{Vi} \quad (20)$$

The purpose of this controller is to achieve a rapid actuation of the control with respect to input variations, both $H_{Vi}(s)$ filters and anti-aliasing filters. Therefore, no significant delays should be generated in the acquisition voltage of the input voltage so as not to generate delays in the time of the control operation.

In this work, the proof of the performance of the feedforward control will be based only on simulation. Thus, all gains will be represented as a single gain of 0.5 (Equations 21 and 21) and the reference voltage will be 48V.

$$H_{Vi}(s) \cdot K_{AD} \cdot K_{Vi} = 0,5 \quad (21)$$

$$V_{ref} = V_{o_projeto} = 0,5 \cdot V_{i_nominal} \quad (22)$$

The transfer function of the $G_{Vi}(k)$ controller, Equation 23, represents the change portion to be given in the preference for the PWM modulator.

$$G_{Vi}(k) = \frac{V_{ref}(k) - V_{Vi}(k)}{V_{Vi}(k)} \quad (23)$$

The $G_{Vi}(k)$ signal in the PWM modulator inserts a delay in the control signal that is applied in the Buck converter. With this, there is oscillation in the output voltage of the converter. The oscillation in the output voltage of the converter is smaller and damping faster than if the system were operating only with the feedback loop based on the output voltage of the converter.

With the operation of the feedforward control, the cyclic ratio applied to the converter will change. However, it is worth remembering that, according to Equation 6, the modeling of the Buck converter depends on the cyclic ratio. The model of the plant changes during the operation of the control, which requires that the control adapts to the new condition of the plant; that is, the control acquires the characteristic of an adaptive control. Although the feedforward controller designed does not depend directly on the plant model and the output variable, its correct sizing predicts that the plant is constant and known. In the case of the PI controller design with feedback control mesh, this depends directly on the plant model and must be recalculated to each control iteration loop based on the data from the current model (or the iteration loop that has just been executed). Failure to adapt the controller to the new situation may cause the system to exhibit a different response characteristic.

The change in the Buck converter model due to change in the cyclic ratio occurs basically in the input matrix or control (Equations 24, 25, and 26) [18,19].

$$\Gamma = \Psi \cdot B \quad (24)$$

Where:

$$\Psi = I \cdot T_s + \frac{A \cdot T_s^2}{2!} + \frac{A^2 \cdot T_s^3}{3!} + \dots + \frac{A^i \cdot T_s^{i+1}}{(i+1)!} \quad (25)$$

Truncating the series in the first 3 terms of Equation 25, the scheme is then:

$$\Gamma = \begin{bmatrix} 0,0370 \cdot d \\ -0,4383 \cdot d \end{bmatrix} \quad (26)$$

5. CONTROLLER VALIDATION AND RESULTS

The controller validation process begins by analyzing the performance of the feedforward controller. The system was simulated in MATLAB according to the equations of state of the Buck converter. The input disturbances were inserted into the input signal V_i after the system was previously operating in steady state. In the simulation, the variations in the input voltage were added instantly at 0.02 seconds in the form of steps (new operating points). For the verification of the behavior of the closed-loop system, a signal in sinusoidal form (continuous disturbances) was used.

Figure 9 represents the closed-loop system response for the output voltage V_o and cyclic ratio d considering the input V_i with disturbances in the form of steps. The cyclic ratio d can be interpreted as the control effort applied to the system.

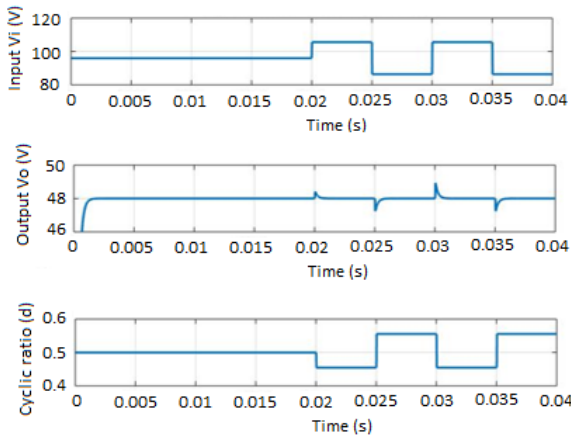


Figure 9 - Closed-loop system response for V_o and d outputs with disturbances in the form of steps.

Figure 10 represents the closed loop system response for the output voltage V_o and cyclic ratio d considering the input V_i with sinusoidal perturbations.

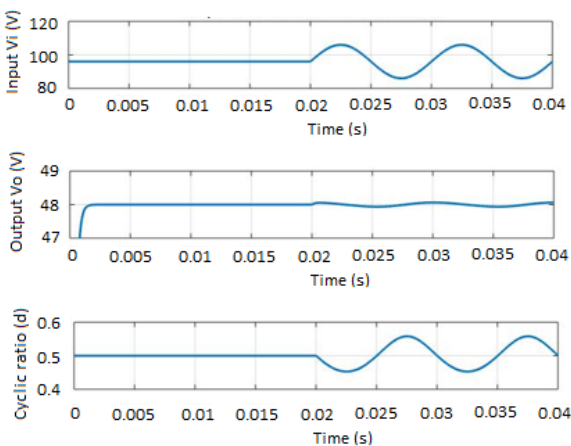


Figure 10 - Closed-loop system response for the V_o and d with sinusoidal perturbation outputs.

In Figure 9 it is verified that the output voltage reaches stability after a brief transient moment in the case of disturbances in the form of steps. In this case, the voltage oscillation is quite low, about 1V or less, that is, within the oscillation limit of the output voltage specified in the design. In Figure 10, it can be seen that the system does not reach a stable output voltage again while the input disturbance does not end, although the rejection ratio to the disturbance is quite high. In the latter case, this non-stabilization is basically due to the type of controller specified to perform the feedforward control. According to the literature, the resonant type controllers are the most indicated to perform the rejection of sinusoidal signals [17].

Figures 11, 12, and 13 represent the response of the system to disturbances at the step input respectively for the system working only with the PI controller, with only the feedforward controller, and with both acting together.

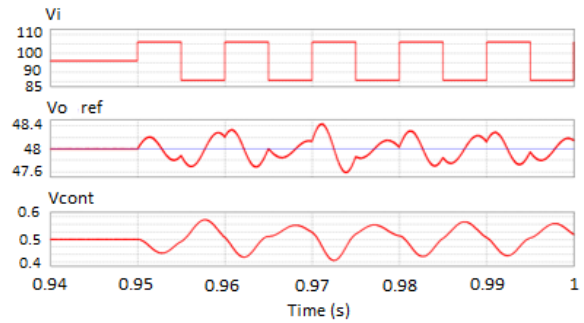


Figure 11 - System response to step disturbances operating only with the PI controller.

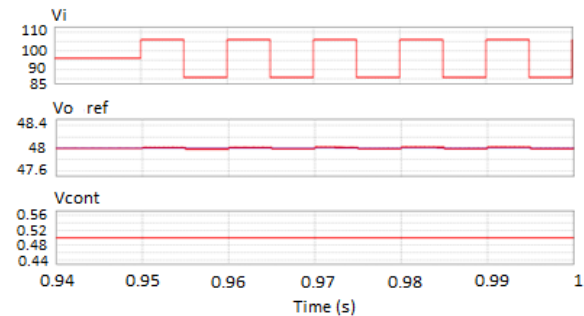


Figure 12 - System response to step disturbances operating only with the forward controller.

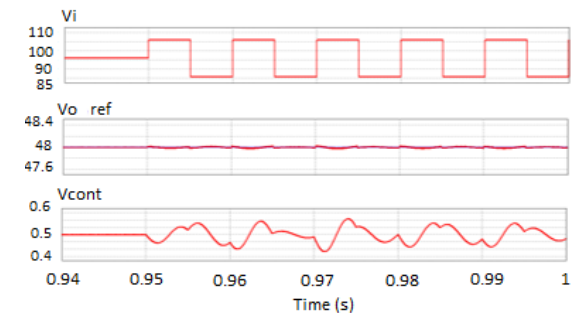


Figure 13 - System response to step disturbances operating with PI and forward controller.

From the results presented, it is verified that only the PI controller cannot bring the system to a new operating regime condition in a timely manner. The junction of both controllers can stabilize the output voltage around an operating point with a minimum output oscillation.

In Figures 14, 15, and 16 the same operating conditions are presented, but with a continuous variation disturbance applied to the input.

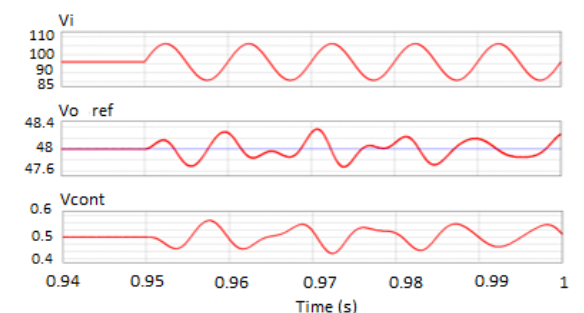


Figure 14 - System response to continuous disturbances operating only with PI controller.

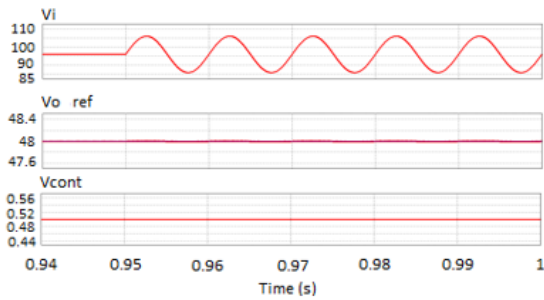


Figure 15 - System response to continuous disturbances operating only with forward controller.

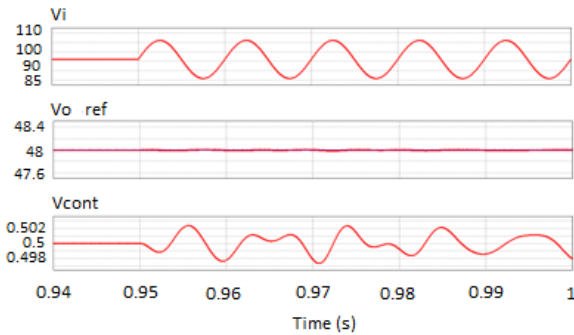


Figure 16 - System response to continuous disturbances operating with PI and forward controller.

For this new operating condition, similar conclusions to operations with step disturbances can be obtained. Only the PI controller in operation exhibits a greater oscillation in the output voltage than both controllers acting together. Regardless of the type of input disturbance, operating the system only as a forward controller is not recommended. In this case the system has some disadvantages: it cannot detect output variations due to changes in load or parametric system, either due to aging of the components, heating, or even variations in the production process. In this way, the joining of both controllers is, from the practical point of view, the best choice.

6. CONCLUSIONS

Although not a commonly published technique for DC-DC converters, control through a feedforward mesh assigns to converters a rejection characteristic to input voltage variations that is extremely interesting. Feedforward mesh presents lower amplitude and accommodation time when compared to the classic control strategies based on output voltage feedback meshes.

The use of this control mesh implies a greater complexity in the elaboration of the software of the microprocessor that will manage the structure. In addition, it implies more hardware resources such as a second A/D converter in the microprocessor or external analog multiplexer, as well as a sensor for the input voltage of the converter.

The validation of the operation of the feedforward control mesh was based purely on models implemented in the PSIM simulation software through system transfer functions.

The design data of the feedback loop and the $G_c(z)$ controller were used only for the comparison of the dynamic response of the disturbance rejection in the input voltage with the feedforward mesh.

REFERENCES

- [1] Dileep, G.; Singh, S.N. Selection of non-isolated DC-DC converters for solar photovoltaic system. *Renewable and Sustainable Energy Reviews*. 76 (2017), p. 1230–1247.
- [2] EL Fadil, H.; Giri, F.; Ahmed-Al, T.; Gaouzi, K. Stability analysis of nonlinear digital control of DC-DC boost power converters with dynamical feedback. *IFAC – Conference Paper Archive*. 49-13 (2016), p. 211-216.
- [3] Zhanga Guidong; Zhong Lib; Bo Zhangc; Wolfgang A. Halangb. *Power electronics converters: Past, present and future*. *Renewable and Sustainable Energy Reviews* 81 (2017) p. 2028–2044.
- [4] Cristri, A.W.; Iskandar, R.F. Analysis and Design of Dynamic Buck Converter with Change in Value of Load Impedance. *Procedia Engineering (Engineering Physics International Conference, EPIC 2016)*. 170 (2017), p. 398 – 403.
- [5] Erickson, R. W.; Maksimović, Dragan. *Fundamentals of Power Electronics*. Kluwer Academic Publishers, 2nd ed. New York, 2004.
- [6] Barbi, Ivo; Martins, Denizar Cruz. *Conversores CC-CC Básicos Não Isolados*. 2^a ed. rev. Florianópolis, 2006.
- [7] F. Alongea; M. Pucci; R. Rabbeni; G. Vitale. Dynamic modelling of a quadratic DC/DC single-switch boost converter. *Electric Power Systems Research*. 152 (2017), p. 130–139.
- [8] T. Arunkumari, V. Indragandhi. An overview of high voltage conversion ratio DC-DC converter configurations used in DC micro-grid architectures. *Renewable and Sustainable Energy Reviews*. 77 (2017) p. 670–687.
- [9] Modabbernia, Mohammad Reza. An Improved State Space Average Modelo of Buck DC-DC Converter with all of the System Uncertainties. *IJEEL*, v.5, n. 1, p. 81-95. 2013.
- [10] Ghosh, Antip; Kandpal, Mayank. *Space State Average Modelo f DC-DC Converters with Parasitic in Discontinuous Conduction Mode (DCM)*. National Institute of Technology, Roukkela, India, 2010.
- [11] DORF, Richard C.; BISHOP, Robert H. *Sistemas de controle modernos*. 11 ed. Rio de Janeiro: LTC, 2009.
- [12] Ogata, K. *Engenharia de Controle Moderno*. 5 ed. São Paulo: Pearson Prentice Hall, 2010.
- [13] Redl, Richard. *Feedforward Control of Switching Regulators*. Em: Steyaert M., van Roermund A., Baschiroto A. (eds) *Analog Circuit Design*. Springer: Dordrecht, 2012.
- [14] Nikolaus Euler-Rollea; Martin Fuhrmann; Markus Reinwaldb; Stefan Jakubeka. Longitudinal tunnel ventilation control. Part 1: Modelling and dynamic feedforward control. *Control Engineering Practice*. 63 (2017), p. 91–103.
- [15] J.L. Guzmána; T. Hägglundb; M. Veronesi; A. Visioli. Performance indices for feedforward control. *Journal of Process Control*. 26 (2015), p. 26–34.
- [16] Lucas, Ricardo. *Análise e Implementação de Estruturas de Controle em Dispositivo FPGA Aplicadas a um Conversor Buck*. Dissertação de Mestrado. UTFPR. Ponta Grossa, 2015.
- [17] Saban Ozdemir. Z-source T-type inverter for renewable energy systems with proportional resonant controller. *International Journal of Hydrogen Energy*. 41 (2016). P. 12591 e 12602.
- [18] Fadali, M. Sami; Visioli, Antonio; *Digital Control Engineering – Analysis and Design*. 2a ed. EUA: Elsevier, 2013.
- [19] Astrom, Karl J.; Wittenmark, Bjorn. *Computer-Controlled Systems – Theory and Design*. 3a ed. China: Prentice Hall, 1997.